

Learning Semantic Segmentation with Query Points Supervision on Aerial Images

Santiago Rivier, Carlos Hinojosa, Silvio Giancola, Bernard Ghanem
King Abdullah University of Science and Technology (KAUST)

santiago.rivier@gmail.com, {carlos.hinojosamontero, silvio.giancola, bernard.ghanem}@kaust.edu.sa

Abstract

Semantic segmentation is crucial in remote sensing, where high-resolution satellite images are segmented into meaningful regions. Recent advancements in deep learning have significantly improved satellite image segmentation. However, most of these methods are typically trained in fully supervised settings that require high-quality pixel-level annotations, which are expensive and time-consuming to obtain. In this work, we present a weakly supervised learning algorithm to train semantic segmentation algorithms that only relies on query point annotations instead of full mask labels. Our proposed approach performs accurate semantic segmentation and improves efficiency by significantly reducing the cost and time required for manual annotation. Specifically, we generate superpixels and extend the query point labels into those superpixels that group similar meaningful semantics. Then, we train semantic segmentation models, supervised with images partially labeled with the superpixels pseudo-labels. We benchmark our weakly supervised training approach on an aerial image dataset and different semantic segmentation architectures, showing that we can reach competitive performance compared to fully supervised training while reducing the annotation effort.

1. Introduction

Semantic segmentation is a critical task in remote sensing and computer vision, where the goal is to assign a class label to each pixel in an image. In particular, semantic segmentation of satellite and aerial images could be incredibly helpful for urban planning, disaster recovery, autonomous agriculture, environmental monitoring, and many others. The ability to accurately segment images into meaningful regions is crucial to derive insights from the vast amount of raw data collected by satellites and airborne sensors. With the advent of deep learning-based methods, the accuracy of supervised semantic segmentation on satellite and aerial images has significantly improved. Some recent works for

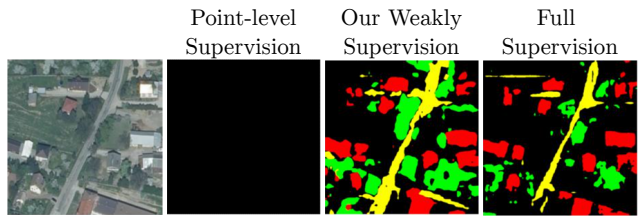


Figure 1. **Weakly Supervised from Query Points for Semantic Segmentation.** Our approach utilizes query point labels for training semantic segmentation algorithms. We extend these annotations to superpixels, capturing spatial contextual information. Our Weakly Supervised Learning (WSL) method balances annotation efficiency and segmentation performance.

semantic segmentation include SegNet [3], FCN [17], U-NET [28], or PSPNet [44] with excellent results in satellite imagery [2, 20, 32].

Typically, these methods require large amounts of pixel-level annotations to supervise from, which are costly and time-consuming to collect. To address the challenge of limited labeled data, methods relying on weaker types of labels appeared, namely Weakly Supervised Learning (WSL). These methods leverage weaker forms of annotations, such as bounding-box annotations [15, 23], scribbles [41, 16, 38], points [4], or simple image-level class labels [22, 26] to infer the segmented regions. In general, these approaches can be especially promising in the field of remote sensing, due to the impracticality of collecting dense pixel-level labels for vast amounts of satellite and aerial images. However, training models with very few supervised pixels poses a significant challenge in correctly identifying the spatial extent of objects in the image. Specifically, the model could only focus on a small section of the target object, resulting in incomplete or inaccurate segmentation. Furthermore, it could also predict all pixels as part of the background class, leading to a false negative prediction [4].

In this work, we propose an efficient semantic segmentation approach requiring a few pixel-level annotations. To overcome the limitations of point-based WSL methods, we lift point annotations to superpixels, embedding consistent

semantic information into spatial context, offering stronger supervision. Fig 1 shows different supervision levels: point-based, partial mask, and full mask annotations. Our method yields comparable results to fully supervised approaches, reducing annotation effort while maintaining high segmentation accuracy. This achieves a better trade-off between annotation efficiency and segmentation performance.

Contributions. We summarize them as follows: (i) We define a novel learning paradigm for satellite image semantic segmentation that only considers point annotations. (ii) We present a novel methodology for weakly annotated settings, that extends labels from points to superpixels and trains on partially annotated superpixels with a masked weighted loss function. (iii) We provide a comprehensive analysis of our WSL approach, showing its capability on different datasets and different model architectures.

2. Related Work

Satellite image understanding is a pivotal field with extensive implications across numerous industries, including agriculture, disaster management, environmental monitoring, and urban planning [43]. One of the critical tasks in satellite image understanding is semantic segmentation, which involves dividing an image into different regions and assigning semantic labels to each segment [17, 4]. This task is essential in identifying and classifying different land covers, such as forests, crops, and water bodies, which can aid in monitoring the state of the environment and informing policy decisions. In this section, we review some related works that address the problem of semantic segmentation for satellite imagery through different approaches, including supervised, unsupervised, and weakly supervised methods, each with advantages and limitations.

Fully-Supervised Semantic Segmentation. Traditional methods extract spectral and spatial information via a pre-processing step and rely on traditional supervised algorithms like SVM [30], MRF [36], and KNN [14]. In recent years, with the blooming of deep learning techniques for extensive data analysis, several deep neural networks have been developed to extract high-level features of satellite images achieving state-of-the-art supervised semantic segmentation performance [45, 43]. One early approach is the fully-convolutional neural networks (FCNs) [17], which have demonstrated promising results in semantic segmentation tasks on natural images. However, FCN is not sensitive to image details and does not consider the relationship between pixels, lacking spatial consistency. Other methods include U-Net [28, 24, 27, 37] and DeepLabV3 [8, 9], which can be adapted to suit the unique characteristics of satellite images, such as their high-resolution and multi-spectral nature. Among recent works, Yin *et al.* [42] proposed to address the loss of context information in semantic seg-

mentation by combining the self-attention mechanism with convolutional neural networks (CNNs) to extract multiscale features and guide local image patches to focus on different objects. Sun *et al.* [35] proposed a new end-to-end fully convolutional segmentation network that is composed of several residual blocks to facilitate convergence. The proposed strategy improves the diversity of spatial land-cover distributions, leading to superior generalization capabilities. The success of such deep learning approaches hinges on a large amount of labeled datasets [10, 34, 5]. In particular, while satellite images are readily obtainable, the efforts to generate high-quality datasets are limited by the enormous effort required to create accompanying annotations, which are not always available and often prohibitively expensive to acquire. To address these challenges, researchers have proposed alternative approaches, such as unsupervised and weakly-supervised semantic segmentation, which may require fewer labeled examples and potentially lead to model with more generalization capabilities.

Unsupervised Semantic Segmentation. Among the learning approaches for semantic segmentation, unsupervised learning is the most challenging as it involves identifying and labeling different objects and regions in satellite images without relying on pre-existing labeled datasets. Generally, the methods in this category aim to discover meaningful patterns and structures in satellite imagery. Recent advances in unsupervised satellite image segmentation include fast subspace clustering [11, 12, 13, 19] and deep clustering approaches [6, 7, 29]. For example, authors in [13] propose a fast algorithm that obtains a sparse representation coefficient matrix by first selecting a small set of pixels that best represent their neighborhood. Then, the algorithm performs spatial filtering to enforce the connectivity of neighboring pixels and uses fast spectral clustering to get the final clustering map. In a more recent work [29], authors propose a novel unsupervised satellite image segmentation that relies on deep clustering and contrastive learning. Specifically, the method samples smaller unlabeled patches from the scene. For each patch, an alternate view is generated by simple transformations, *e.g.* the addition of noise. Both views are then processed through a two-stream network, and weights are iteratively refined using deep clustering, spatial consistency, and contrastive learning in the pixel space. Although unsupervised semantic segmentation algorithms do not require any labeled data, they are generally less accurate than supervised approaches as they may not capture the high-level semantic meaning of the image.

Weakly Supervised Semantic Segmentation. Unlike traditional supervised learning methods that require pixel-level annotations for every image, weakly-supervised segmentation relies on less precise annotations such as point-level labels [4], image-level labels [1], scribbles [40] or bounding boxes [15]. Weakly supervised methods are gener-

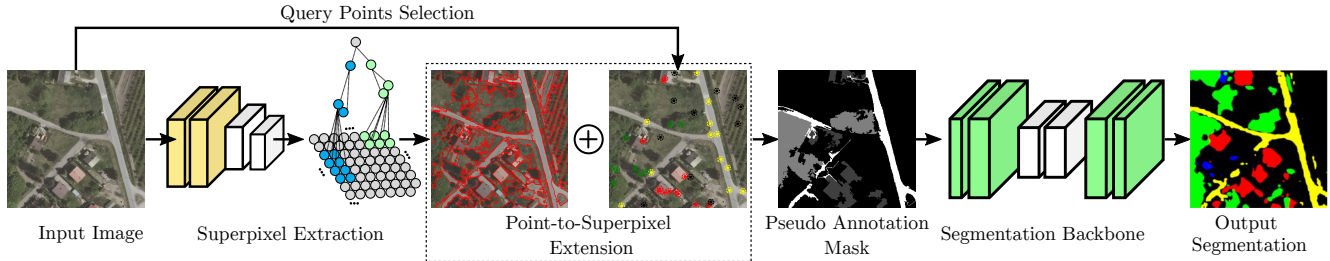


Figure 2. **Proposed WSL Approach for Semantic Segmentation on Aerial Images.** Our approach solely considers query point-based annotation on satellite images and relies on superpixel extraction[25] to extend the point-based annotation into larger regions. We minimize our proposed masked loss by leveraging the generated partial mask pseudo-annotations, which provide more supervisory signals than the sole query point-based annotations.

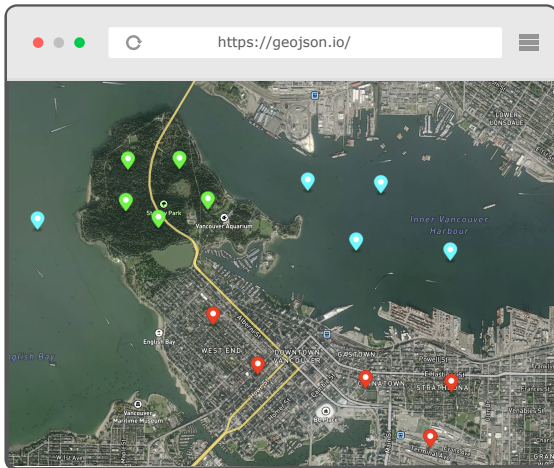


Figure 3. **Query Points Selection.** Our approach only requires users to select query points to segment the land cover.

ally more accurate than unsupervised ones and less accurate than supervised approaches. Wang *et al.* [39] explore weak labels in the form of a single-pixel label per image and class activation maps to perform semantic segmentation on satellite images. Nivaggioli *et al.* [21] adopted the method proposed in [1] to perform semantic segmentation on satellite imagery. Similarly, Schmitt *et al.* [31] adopted DeepLabv3+[8, 9], and U-Net DL-based [28] models have been employed along with pixel-level image fusion to conduct semantic segmentation of the satellite images. One issue with training models with very few or no supervised pixels is correctly inferring the spatial context of the objects. In general, weakly supervised methods are prone to local minima: focusing on only a small part of the target object or predicting all pixels as belonging to the background class [4]. In this work, we leverage point-based annotations along with superpixels to train semantic segmentation algorithms. Specifically, we extend the point annotations into superpixels and generate a partial mask to supervise from. We optimize our end-to-end framework using a pretrained segmentation backbone and finetune it with our proposed

masked loss to particularly learn from the points selected by the user.

3. Methodology

We present a novel end-to-end framework for satellite image semantic segmentation, as shown in Figure 2. The method utilizes user-selected query points P as the sole source of supervision for the task. The framework consists of three stages: superpixel extraction, pseudo-mask generation by expanding point annotations into superpixels, and the segmentation module. The segmentation module, a pre-trained backbone, is fine-tuned with our proposed masked loss. Below, we elaborate on each component of our approach.

3.1. Point selection

Our semantic segmentation algorithm requires an image and a set of query points as input. These query points can be conveniently selected using online tools like <https://geojson.io/> (see Fig 3). To facilitate experimentation and validation, we developed an algorithm to position P points within the images. Each point’s spatial placement allows us to assign the corresponding label based on the ground truth, simulating the manual labeling process efficiently. Two distinct methods are used: random points per image and random points per label. In the first method, labels are assigned to images using random points, with the probability of a class being labeled proportional to its dataset imbalance. However, this method may lose information for imbalanced datasets. In contrast, the second method evaluates the number of classes in each image and distributes the required points equally among the classes. This approach ensures accurate annotation for imbalanced classes.

3.1.1 Superpixel

In this work, we adopt the DAL-HERS [25] superpixels algorithm to generate the superpixel regions shown in Fig. 2.

DAL-HERS is a deep learning-based technique that computes affinities between neighboring pixels. Specifically, the algorithm is based on a hierarchical merging approach, where neighboring regions are merged into larger superpixels based on their affinities. The affinities between neighboring pixels are computed using a deep neural network trained to predict the probability of pixel pairs belonging to the same superpixel. The network considers the image’s color and texture information to compute the affinities. The merging process is guided by the hierarchical entropy rate [25], which measures the complexity of the image at different scales. The algorithm seeks to minimize the hierarchical entropy rate by merging neighboring superpixels with high affinities. Formally, let’s denote as S the superpixel region generated by DAL-HERS. Then, the assignment of labeled key points L_p in the corresponding superpixel region can be expressed as:

$$L_s = \begin{cases} \text{mode}(L_p), & \text{if } \exists p \in P \text{ such that } p \in S \\ \text{no label}, & \text{otherwise} \end{cases}$$

Here, the mode of L_p is calculated to determine the label with the highest number of points within that superpixel region. In the case of a multimode result where two labels have an equal number of points, no label is assigned to that superpixel.

3.1.2 Weakly Supervised Training from Superpixel

To generate the pseudo-annotations mask, we need to merge the query points selected by the user with the superpixels regions. Here, the objective is to extend the point-level annotations to regions considering the spatial contextual information. The underlying logic of our approach is that if we have a superpixel region with one point labeled, we propagate this label in all this region. However, in the same superpixel region, it could be possible to have more than one point since the performance of the superpixel algorithm when detecting the image boundaries is not perfect. Therefore, it is possible to have more than two labels in the same superpixel region when looking at the ground truth. To solve this, we count the number of points by each class and propagate the class with the most points. For the rest of the regions which do not contain any query points, we assign such points to the background class.

3.1.3 Weighted Masked Loss

We propose a novel weighted masked loss to train our proposed approach and leverage the supervisory signals provided by the generated pseudo-annotations mask. This loss function consists of a Mean Square Error (MSE), which we multiply with a binary mask that contains one where the image is labeled and zero where the image is unlabeled. With

this approach, we consider only the pixels with labels during our optimization process. Also, this loss function corrects the class imbalance by dividing the masked loss by the percent of each class, penalizing the classes with the highest percentage. Formally, we define our proposed weighted masked loss as:

$$\mathcal{L} = \frac{1}{N} \sum l_i = \frac{1}{N} \sum_{i=1}^N \left(\frac{1}{C} \sum_{c=1}^C [m_{i,c} \cdot (wl_{i,c} - pl_{i,c})^2] \right)$$

where N corresponds to the batch size; l_i is the loss by sample, C is the number of classes; $m_{i,c}$ is the binary mask value for class c and image sample i ; $wl_{i,c}$ is the weakly supervised label; and $pl_{i,c}$ is the predicted label. Note that the variable $pl_{i,c}$ represents the estimated label, and is clarified the use of one-hot encoding for class representation. During training, we use our loss \mathcal{L} with different semantic segmentation models and feature extractor backbones; see Section 4.

4. Experiments

4.1. Experimental Setup

Datasets. We evaluated our proposed weakly supervised semantic segmentation approach using the LandCoverAI dataset [5]. This dataset comprises images extracted from aerial photos used to create a digital orthophoto of Poland. The images are drawn from a public geodetic resource and were used to update the reference data of the land parcel identification system (LPIS). Captured with a spatial resolution of 25 or 50 cm per pixel, the images contain three spectral bands (RGB) and span from 2015 to 2018. They were taken from various flights, providing diverse optical conditions, including different saturation levels, sunlight angles, shadow lengths, and various vegetation seasons. The dataset consists of 41 orthophoto tiles manually selected from counties across Poland, with each tile covering approximately 5 km² area. There are 33 images with a resolution of 25 cm (approximately 9000 x 9500 px) and eight images with a resolution of 50 cm (approximately 4200 x 4700 px), resulting in a total coverage of 216.27 km².





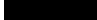
Class name	Color
Woodland	
Building	
Road	
Water	
Background	

Figure 4. Color Legend of Classes.

The LandCoverAI dataset includes four classes: *buildings* (1), *woodland* (2), *water* (3), and *road* (4). A *building* annotation includes the roof and visible walls, while *woodland* denotes land covered with multiple trees. *Water* encompasses both flowing and stagnant water bodies,

excluding ditches and dry riverbeds. The *road* annotation includes roads, parking areas, unpaved roads, and tracks. Lastly, the *background* class represents areas not classified into any of the above classes, which may include fields, grass, pavements, etc. This work uses TorchGeo [33] to load and preprocess the LandCoverAI images. TorchGeo is a PyTorch domain library, similar to torchvision, providing datasets, samplers, transforms, and pre-trained models specific to geospatial data. In this case, TorchGeo provided us with 10674 images of size 512×512 , which we split into 60% for training, 20% for validation, and 20% for testing.

Models. In principle, any semantic segmentation backbone can be used within our framework, as illustrated in Figure 2. In our experiments, we tested three main architectures.

FCNet [18] stands for *Fully Convolutional Network* and is a well-known architecture to perform semantic segmentation. The main advantage of FCNet is that it can accept inputs of arbitrary size and produce correspondingly-sized output with efficient inference and learning. The architecture of FCNet employs solely locally connected layers, such as convolution, pooling, and upsampling. Avoiding the use of dense layers means fewer parameters, making the networks faster to train. The network consists of a downsampling path, used to extract and interpret the context, and an upsampling path, which allows for localization. FCNs also employ skip connections to recover the fine-grained spatial information lost in the downsampling path.

UNet [28] is a neural network named after its U-shape design, comprising a contracting path and an expansive path. The contracting path, similar to a typical convolutional neural network, involves convolutional and pooling layers to gradually reduce the spatial dimensions and capture global context and high-level features. Conversely, the expansive path employs upsampling and convolutional layers to progressively increase the feature map’s spatial dimensions, integrating it with the feature maps from the contracting path. This process refines the segmentation mask by combining local information with a global context. An essential aspect of UNet is its skip connections, facilitating the fusion of feature maps from the contracting and expansive paths. This enables the network to capture both local and global information, contributing to accurate segmentation. Moreover, these skip connections help address the problem of information loss during downsampling.

DeepLabV3[8, 9] is a family of convolutional models designed for semantic segmentation tasks. DeepLabV3 uses a modified version of the atrous convolution, also known as dilated convolution, to extract features at multiple scales from the input image. The DeepLabV3 architecture incorporates a backbone to extract complex features from the input image. In this work, we explore the combination of DeepLabV3 with ResNet50 and ResNet101 networks as backbones to see its impact on our weakly supervised se-

matic segmentation approach. The extracted features from the input image are then passed through a series of convolutional and pooling layers to reduce the spatial resolution of the feature maps. The resulting feature maps are then fed into the atrous convolutional module of DeepLabV3 to extract features at multiple scales. Finally, the resulting features are fed into a classifier that produces a segmentation mask, where each pixel is assigned a label indicating its corresponding class.

Metrics. To measure the performance of our proposed framework, this work uses the mean Intersection-Over-Union (mIoU) metric. Here we used the Jaccard index from the PyTorch library. The Jaccard index is a statistic that can be used to determine the similarity and diversity of a sample set. It is defined as the size of the intersection divided by the union of the sample sets:

$$J(A, B) = \frac{|A \cap B|}{|A \cup B|}$$

To configure the parameters of the Jaccard index, we ignore index zero as our loss function is only computed from the labeled regions. Also, the statistics used to calculate the mIoU are set as “micro”, which means that the sum statistics are computed over all labels.

Training details. During training, we fine-tuned various parameters to compare model performances. The learning rate (LR) was set to $1e^{-4}$ with a scheduler that decreased the LR by a factor of 10 at each plateau until convergence. For models trained from scratch, 300 epochs proved sufficient as further epochs did not yield improvements. In some cases, the LR scheduler completed training earlier. For fine-tuned pre-trained models, 40 to 60 epochs achieved accurate predictions. After evaluating batch sizes of 4, 8, 16, and 32, we selected a batch size of 32 for faster training without significant performance differences. The PyTorch implementation of Adam with default parameters served as the optimizer. All training sessions were conducted on a single NVidia V100 GPU.

4.2. Initial Results

As mentioned, only using point-level annotations without contextual spatial information will lead to poor results. Indeed, we initially trained a DeepLabV3 model with point-level supervision. As observed in Fig. 5, if we use only the selected points as input, we observe that DeepLabV3 cannot obtain a proper segmentation mask.

Therefore, as depicted in Fig. 2, by merging the point-level annotations with superpixels information, we observed an improvement in the performance of a standard DeepLabV3 model that had previously yielded suboptimal results for the approach of weakly semantic segmentation, see Fig. 6.

To establish an upper bound of performance, we trained DeepLabV3 with full supervision and attained a mIoU score

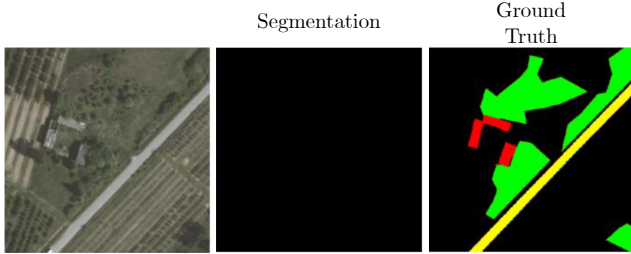


Figure 5. **Segmentation output of point-level supervision.** Training with point-level supervision does not satisfactory.

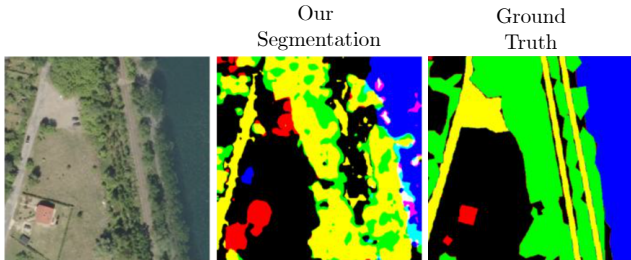


Figure 6. **Segmentation output of superpixel supervision.** Training with superpixel supervision leads to more supervisory signals and better quality semantic segmentation.

of 0.8399. Using this score as our reference point, our goal is to conduct further experimentation through various ablation tests to achieve similar performance.

4.3. Extended Analysis

For conducting the ablation study of our proposed method, we employed the DeepLabV3 architecture as the segmentation backbone. We repeated each experiment five times to ensure reliable and consistent results.

Effect of the Loss. Developing a robust loss function is essential for achieving accurate image segmentation. In our approach, we tested PyTorch’s MSELoss and CrossEntropyLoss with various hyperparameters, but they yielded unsatisfactory results. Therefore, we introduced our weighted masked loss (Section 3) that takes into account the prediction, one-hot encoded label, and label without encoding. By computing the MSE loss only for labeled pixels, we observed significant improvements in our experiments. To understand the impact on uncomputed regions, which may hold crucial information, we compared model performance using completely labeled and weakly labeled data, as depicted in Fig. 7. This analysis shed light on the loss function’s influence on uncomputed regions and overall performance. To address class imbalance, we implemented class balancing by dividing the loss result by the percentage of each class. This approach penalizes high-occurrence classes while rewarding low-occurrence ones, leading to enhanced image segmentation accuracy.

Effect of the number of point labels. Using more query

Table 1. **Multiple ablation studies of our method.** (a) using the DeepLabV3 backbone model with cross-entropy loss and our proposed masked loss; (b) varying the number of points to generate the pseudo annotation mask; (c) varying the number of superpixels after fixing the number of points to 50; and (d) with/without the edge option in DAL-HERS.

Experiment		mIoU
Loss (a)	Cross Entropy	0.5646 ± 0.02
	Masked Loss (Ours)	0.7564 ± 0.01
	Fully Labeled	0.8399 ± 0.01
Point (b)	10	0.6690 ± 0.03
	20	0.7194 ± 0.01
	30	0.7433 ± 0.01
	40	0.7384 ± 0.02
	50	0.7564 ± 0.01
Superpixel (c)	80	0.7543 ± 0.01
	100	0.7564 ± 0.01
	200	0.6983 ± 0.03
	300	0.6967 ± 0.05
Edge (d)	True	0.7527 ± 0.01
	False	0.7564 ± 0.01

points in our framework will conduct in a better pseudo annotation mask which means more level of supervision. Therefore, as observed in Table 1, increasing the number of points will lead to better performance in terms of mIoU.

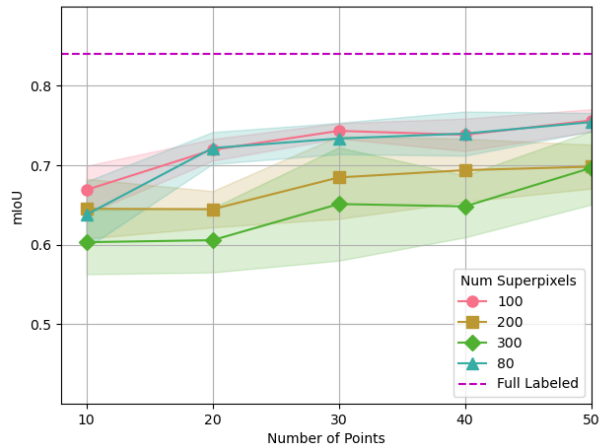


Figure 7. **Segmentation Performances per Number of Points.** We show the performance with different numbers of points for each number of superpixels.

Effect of the Number of Superpixels The number of superpixels employed in our framework significantly influences its performance. A reduction in the number of superpixels results in larger regions while increasing the number of superpixels leads to smaller regions. The operation of

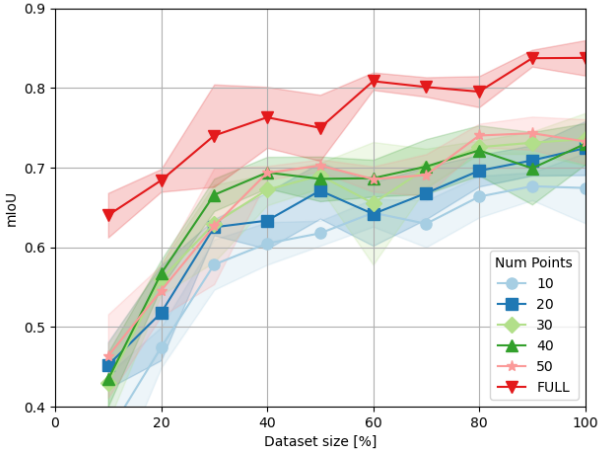


Figure 8. **Segmentation Performances per Dataset Size.** Our results demonstrate that larger datasets lead to improved performance. The experiment was conducted using a dataset of a total amount of 10,674 images.

DAL-HERS imposes a minimum number of superpixels required for successful image segmentation. This minimum threshold is determined empirically and depends on factors such as image size and complexity. For the LandCover dataset used in our study, we found that a minimum of 80 superpixels is necessary. Furthermore, our experimental results, as depicted in Fig. 7, reveal an inverse relationship between the number of superpixels and mIoU. Specifically, an increase in the number of superpixels corresponds to a decrease in mIoU.

Effect of using edge in superpixel. The current superpixel algorithm provides the option of specifying the “edge” hyperparameter to use a border detector and generate more precise superpixel regions. However, the default setting for this parameter is False. In our experiments, we compared the performance of superpixels generated with and without the edge parameter on a dataset of interest. Specifically, we compared the mIoU scores of 100 superpixels with 50 points each in Table 1(d). As observed from the table, there were no significant performance improvements when using the edge parameter.

Performance of our model varying dataset size Here we analyze how the performance of our method changes when varying the dataset size in terms of mIoU. In Fig. 8, we show the relationship between mIoU and the dataset size used in our framework.

Generalization to different segmentation backbones. To evaluate the generalizability of our weakly supervised semantic segmentation approach, we conducted experiments using three widely used semantic segmentation models as backbones: DeepLabV3, U-Net, and FCNet. To better understand the performance of DeepLabV3 and FCNet,

we compared two variants of each backbone: DeepLabV3 with ResNet50 and ResNet101; FCNet with ResNet50 and ResNet101. These comparisons provided valuable insights into each segmentation backbone’s relative strengths and weaknesses and shed light on the impact of different architectures on their performance.

DAL-HERS vs SAM. Although superpixel models are not the primary focus of our work, we also performed a comparative analysis of the *pre-trained* models DAL-HERS and SAM using the same satellite image to assess their segmentation performance. Our findings reveal that DAL-HERS outperforms SAM in segmentation accuracy. Notably, as seen in Fig 9, DAL-HERS demonstrates the ability to avoid segmenting undesired areas, which SAM fails to achieve. More importantly, DAL-HERS provides an accurate segmentation of the boundaries with up to three times faster processing time than SAM. This is a crucial feature of our method, especially when dealing with extensive image datasets.

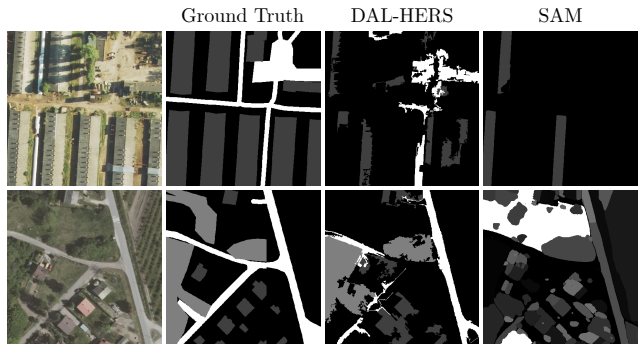


Figure 9. **DAL-HERS vs SAM.** Comparison of outputs of the models DAL-HERS and SAM after labeling the images with points.

Table 2. **Generalization to different segmentation backbones.** Our WSL approach generalizes well across different segmentation backbones (see Fig. 2), with DeepLabV3 performing the best.

Model	mIoU
DeepLabV3 (ResNet50)	0.756 ± 0.01
DeepLabV3 (ResNet101)	0.756 ± 0.02
FCN (ResNet50)	0.728 ± 0.01
FCN (ResNet101)	0.735 ± 0.01
U-Net	0.589 ± 0.02

4.4. Qualitative Results

We show some qualitative results of our approach in Fig. 10. As observed, our weakly supervised semantic segmentation approach generates visually comparable results to costly, fully supervised methods.

4.5. Quantitative Results

Table 1 showcases the quantitative results derived from our experimental analysis. The findings indicate a signifi-

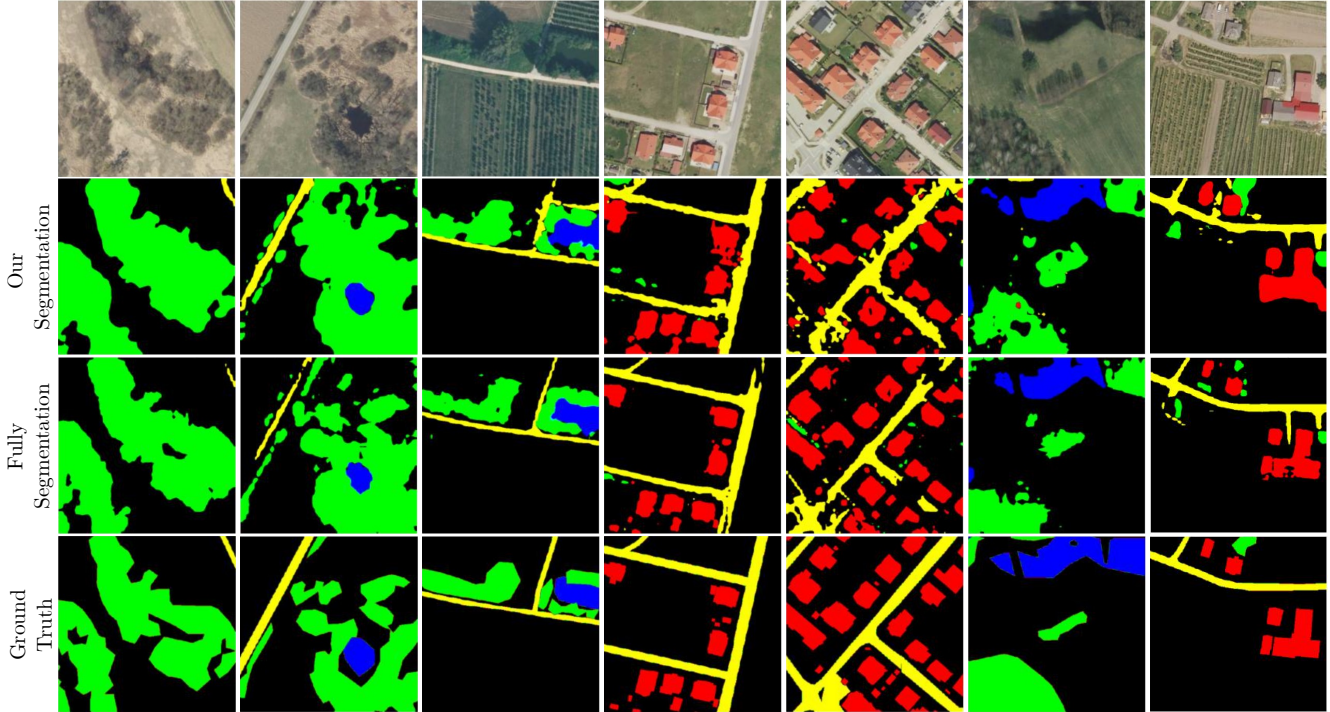


Figure 10. **Qualitative Results on LandCoverAI.** From top to bottom: Satellite Image, weakly supervised results (ours), fully supervised results, and ground truth. Our proposed WSL approach presents visual results comparable to expensive fully supervised setups.

cant reduction in labeling time of over 50%. However, it is important to note that this reduction in time comes at the expense of an 8% decrease in mIoU. Consequently, it is important to analyze the cost-benefit based on the type of application to be implemented.

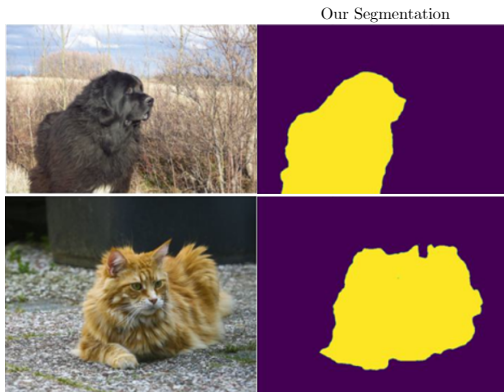


Figure 11. **Qualitative Results on OxfordIIITPet.** From left to right: Input image, ours WSL semantic segmentation. Our training method generalizes to other domains with satisfactory results.

4.6. Domain Generalization

To explore the generalization capability of our framework beyond the geospatial domain, we conducted experiments on the OxfordIIITPet dataset from Torchvision,

which contains 4434 images of cats and dogs. This experiment evaluated whether our framework could be extended to other domains within computer vision. For training, we set the number of superpixels to 300 with the “edge” option and selected 25 points per image. Fig 11 shows some qualitative results of our model. After testing, we obtained a mIoU of 0.8747.

5. Conclusions

In this paper, we presented a novel framework for semantic segmentation that significantly reduces the time and cost required for manual annotation. Our approach achieves high segmentation performance using only point-based annotations, minimizing annotation efforts. Our evaluation across multiple semantic segmentation backbone models and domains demonstrates the effectiveness of our framework in addressing the bottleneck of manual annotation in computer vision. The results of our experiments suggest that our method has practical implications for developing new models and applications where efficient annotation is crucial for success. As future work, we plan to improve our framework by incorporating pixel clustering methods to achieve even greater annotation efficiency. Also, we plan to test our method in other large-scale satellite image datasets and aim to explore our approach’s applicability to new domains to enhance its generalization capability and usability.

References

- [1] Jiwoon Ahn and Suha Kwak. Learning pixel-level semantic affinity with image-level supervision for weakly supervised semantic segmentation. In *Proceedings of the IEEE conference on computer vision and pattern recognition*, pages 4981–4990, 2018. 2, 3
- [2] Nicolas Audebert, Bertrand Le Saux, and Sébastien Lefèvre. Joint learning from earth observation and openstreetmap data to get faster better semantic maps. In *Proceedings of the IEEE Conference on Computer Vision and Pattern Recognition Workshops*, pages 67–75, 2017. 1
- [3] Vijay Badrinarayanan, Alex Kendall, and Roberto Cipolla. Segnet: A deep convolutional encoder-decoder architecture for image segmentation. *IEEE Transactions on Pattern Analysis and Machine Intelligence*, 39(12):2481–2495, 2017. 1
- [4] Amy Bearman, Olga Russakovsky, Vittorio Ferrari, and Li Fei-Fei. What’s the point: Semantic segmentation with point supervision. In *Computer Vision–ECCV 2016: 14th European Conference, Amsterdam, The Netherlands, October 11–14, 2016, Proceedings, Part VII 14*, pages 549–565. Springer, 2016. 1, 2, 3
- [5] Adrian Boguszewski, Dominik Batorski, Natalia Ziembajankowska, Tomasz Dzedzic, and Anna Zambrzycka. Landcover. ai: Dataset for automatic mapping of buildings, woodlands, water and roads from aerial imagery. In *Proceedings of the IEEE/CVF Conference on Computer Vision and Pattern Recognition*, pages 1102–1110, 2021. 2, 4
- [6] Mathilde Caron, Piotr Bojanowski, Armand Joulin, and Matthijs Douze. Deep clustering for unsupervised learning of visual features. In *Proceedings of the European conference on computer vision (ECCV)*, pages 132–149, 2018. 2
- [7] Mathilde Caron, Ishan Misra, Julien Mairal, Priya Goyal, Piotr Bojanowski, and Armand Joulin. Unsupervised learning of visual features by contrasting cluster assignments. *Advances in neural information processing systems*, 33:9912–9924, 2020. 2
- [8] Liang-Chieh Chen, George Papandreou, Florian Schroff, and Hartwig Adam. Rethinking atrous convolution for semantic image segmentation. *arXiv preprint arXiv:1706.05587*, 2017. 2, 3, 5
- [9] Liang-Chieh Chen, Yukun Zhu, George Papandreou, Florian Schroff, and Hartwig Adam. Encoder-decoder with atrous separable convolution for semantic image segmentation. In *Proceedings of the European conference on computer vision (ECCV)*, pages 801–818, 2018. 2, 3, 5
- [10] Ilke Demir, Krzysztof Koperski, David Lindenbaum, Guan Pang, Jing Huang, Saikat Basu, Forest Hughes, Devis Tuia, and Ramesh Raskar. Deepglobe 2018: A challenge to parse the earth through satellite images. In *Proceedings of the IEEE Conference on Computer Vision and Pattern Recognition Workshops*, pages 172–181, 2018. 2
- [11] Carlos Hinojosa, Jorge Bacca, and Henry Arguello. Coded aperture design for compressive spectral subspace clustering. *IEEE Journal of Selected Topics in Signal Processing*, 12(6):1589–1600, 2018. 2
- [12] Carlos Hinojosa, Fernando Rojas, Sergio Castillo, and Henry Arguello. Hyperspectral image segmentation using 3d regularized subspace clustering model. *Journal of Applied Remote Sensing*, 15(1):016508–016508, 2021. 2
- [13] Carlos Hinojosa, Esteban Vera, and Henry Arguello. A fast and accurate similarity-constrained subspace clustering algorithm for hyperspectral image. *IEEE Journal of Selected Topics in Applied Earth Observations and Remote Sensing*, 14:10773–10783, 2021. 2
- [14] Kunshan Huang, Shutao Li, Xudong Kang, and Leyuan Fang. Spectral–spatial hyperspectral image classification based on knn. *Sensing and Imaging*, 17:1–13, 2016. 2
- [15] Anna Khoreva, Rodrigo Benenson, Jan Hosang, Matthias Hein, and Bernt Schiele. Simple does it: Weakly supervised instance and semantic segmentation. In *Proceedings of the IEEE conference on computer vision and pattern recognition*, pages 876–885, 2017. 1, 2
- [16] Di Lin, Jifeng Dai, Jiaya Jia, Kaiming He, and Jian Sun. Scribblesup: Scribble-supervised convolutional networks for semantic segmentation. In *Proceedings of the IEEE conference on computer vision and pattern recognition*, pages 3159–3167, 2016. 1
- [17] Jonathan Long, Evan Shelhamer, and Trevor Darrell. Fully convolutional networks for semantic segmentation. In *Proceedings of the IEEE Conference on Computer Vision and Pattern Recognition (CVPR)*, June 2015. 1, 2
- [18] Jonathan Long, Evan Shelhamer, and Trevor Darrell. Fully convolutional networks for semantic segmentation. In *Proceedings of the IEEE conference on computer vision and pattern recognition*, pages 3431–3440, 2015. 5
- [19] Jhon Lopez, Carlos Hinojosa, and Henry Arguello. Efficient subspace clustering of hyperspectral images using similarity-constrained sampling. *Journal of Applied Remote Sensing*, 15(3):036507–036507, 2021. 2
- [20] Diego Marcos, Michele Volpi, Benjamin Kellenberger, and Devis Tuia. Land cover mapping at very high resolution with rotation equivariant cnns: Towards small yet accurate models. *ISPRS journal of photogrammetry and remote sensing*, 145:96–107, 2018. 1
- [21] Adrien Nivaggioli and Hicham Randrianarivo. Weakly supervised semantic segmentation of satellite images. In *2019 Joint Urban Remote Sensing Event (JURSE)*, pages 1–4, 2019. 3
- [22] Seong Joon Oh, Rodrigo Benenson, Anna Khoreva, Zeynep Akata, Mario Fritz, and Bernt Schiele. Exploiting saliency for object segmentation from image level labels. In *2017 IEEE conference on computer vision and pattern recognition (CVPR)*, pages 5038–5047. IEEE, 2017. 1
- [23] George Papandreou, Liang-Chieh Chen, Kevin P Murphy, and Alan L Yuille. Weakly-and semi-supervised learning of a deep convolutional network for semantic image segmentation. In *Proceedings of the IEEE international conference on computer vision*, pages 1742–1750, 2015. 1
- [24] Dhanishtha Patil, Komal Patil, Rutuja Nale, and Sangita Chaudhari. Semantic segmentation of satellite images using modified u-net. In *2022 IEEE Region 10 Symposium (TEN-SYMP)*, pages 1–6, 2022. 2
- [25] Hankui Peng, Angelica I Aviles-Rivero, and Carola-Bibiane Schönlieb. Hers superpixels: Deep affinity learning for hierarchical entropy rate segmentation. In *Proceedings of the*

- IEEE/CVF Winter Conference on Applications of Computer Vision*, pages 217–226, 2022. 3, 4
- [26] Pedro O Pinheiro and Ronan Collobert. From image-level to pixel-level labeling with convolutional networks. In *Proceedings of the IEEE conference on computer vision and pattern recognition*, pages 1713–1721, 2015. 1
- [27] Vasilis Pollatos, Loukas Kouvaras, and Eleni Charou. Land cover semantic segmentation using resunet. *arXiv preprint arXiv:2010.06285*, 2020. 2
- [28] Olaf Ronneberger, Philipp Fischer, and Thomas Brox. U-net: Convolutional networks for biomedical image segmentation. In *Medical Image Computing and Computer-Assisted Intervention—MICCAI 2015: 18th International Conference, Munich, Germany, October 5-9, 2015, Proceedings, Part III 18*, pages 234–241. Springer, 2015. 1, 2, 3, 5
- [29] Sudipan Saha, Muhammad Shahzad, Lichao Mou, Qian Song, and Xiao Xiang Zhu. Unsupervised single-scene semantic segmentation for earth observation. *IEEE Transactions on Geoscience and Remote Sensing*, 60:1–11, 2022. 2
- [30] Karen Sanchez, Carlos Hinojosa, and Henry Arguello. Supervised spatio-spectral classification of fused images using superpixels. *Applied optics*, 58(7):B9–B18, 2019. 2
- [31] Michael Schmitt, Jonathan Prexl, Patrick Ebel, Lukas Liebel, and Xiao Xiang Zhu. Weakly supervised semantic segmentation of satellite images for land cover mapping—challenges and opportunities. *arXiv preprint arXiv:2002.08254*, 2020. 3
- [32] Jamie Sherrah. Fully convolutional networks for dense semantic labelling of high-resolution aerial imagery. *arXiv preprint arXiv:1606.02585*, 2016. 1
- [33] Adam J. Stewart, Caleb Robinson, Isaac A. Corley, Anthony Ortiz, Juan M. Lavista Ferres, and Arindam Banerjee. TorchGeo: Deep learning with geospatial data. In *Proceedings of the 30th International Conference on Advances in Geographic Information Systems, SIGSPATIAL '22*, pages 1–12, Seattle, Washington, 11 2022. Association for Computing Machinery. 5
- [34] Gencer Sumbul, Marcela Charfuelan, Begüm Demir, and Volker Markl. Bigearthnet: A large-scale benchmark archive for remote sensing image understanding. In *IGARSS 2019 - 2019 IEEE International Geoscience and Remote Sensing Symposium*, pages 5901–5904, 2019. 2
- [35] Hao Sun, Xiangtao Zheng, and Xiaoqiang Lu. A supervised segmentation network for hyperspectral image classification. *IEEE Transactions on Image Processing*, 30:2810–2825, 2021. 2
- [36] Yuliya Tarabalka, Mathieu Fauvel, Jocelyn Chanussot, and Jón Atli Benediktsson. Svm-and mrf-based method for accurate classification of hyperspectral images. *IEEE Geoscience and Remote Sensing Letters*, 7(4):736–740, 2010. 2
- [37] Priit Ulmas and Innar Liiv. Segmentation of satellite imagery using u-net models for land cover classification. *arXiv preprint arXiv:2003.02899*, 2020. 2
- [38] Paul Vernaza and Manmohan Chandraker. Learning random-walk label propagation for weakly-supervised semantic segmentation. In *Proceedings of the IEEE conference on computer vision and pattern recognition*, pages 7158–7166, 2017. 1
- [39] Sherrie Wang, William Chen, Sang Michael Xie, George Azari, and David B Lobell. Weakly supervised deep learning for segmentation of remote sensing imagery. *Remote Sensing*, 12(2):207, 2020. 3
- [40] Yao Wei and Shunping Ji. Scribble-based weakly supervised deep learning for road surface extraction from remote sensing images. *IEEE Transactions on Geoscience and Remote Sensing*, 60:1–12, 2021. 2
- [41] Weimin Wu, Huan Qi, Zhenrui Rong, Liang Liu, and Hongye Su. Scribble-supervised segmentation of aerial building footprints using adversarial learning. *IEEE Access*, 6:58898–58911, 2018. 1
- [42] Peng Yin, Dongmei Zhang, Wei Han, Jiang Li, and Jianmei Cheng. High-resolution remote sensing image semantic segmentation via multiscale context and linear self-attention. *IEEE Journal of Selected Topics in Applied Earth Observations and Remote Sensing*, 15:9174–9185, 2022. 2
- [43] Lefei Zhang and Liangpei Zhang. Artificial intelligence for remote sensing data analysis: A review of challenges and opportunities. *IEEE Geoscience and Remote Sensing Magazine*, 10(2):270–294, 2022. 2
- [44] Hengshuang Zhao, Jianping Shi, Xiaojuan Qi, Xiaogang Wang, and Jiaya Jia. Pyramid scene parsing network. In *Proceedings of the IEEE conference on computer vision and pattern recognition*, pages 2881–2890, 2017. 1
- [45] Xiao Xiang Zhu, Devis Tuia, Lichao Mou, Gui-Song Xia, Liangpei Zhang, Feng Xu, and Friedrich Fraundorfer. Deep learning in remote sensing: A comprehensive review and list of resources. *IEEE geoscience and remote sensing magazine*, 5(4):8–36, 2017. 2